**Engineering and Technology Journal**
**Journal homepage:** https://etj.uotechnology.edu.iq

# Antenna Gain-Bandwidth Enhancements Using CRLH Hilbert Fractal-based Structure

**Marwa M. Ismail**[a], **Taha A. Elwi**[b]*, **A. J. Salim**[a]

[a]Electrical Engineering Dept., University of Technology-Iraq,Alsina'a street,10066 Baghdad, Iraq.
[b]Communication Engineering Dept., Al-Ma'moon University College, Baghdad, Iraq
*Corresponding author Email: Taelwi82@gmail.com

## HIGHLIGHTS

- This paper introduces the design of low-profile metamaterial-based arrays.
- The array unit cell comprises a CRLH unit cell. A third-order Hilbert curve structure replaces the VIA, and aperiodic slots are introduced between the unit cells to enhance the overall performance.
- A dual- bandwidth was achieved extended from (3.72 to 3.79) GHz and (6.99 to 8.55) GHz with maximum antenna gain equal to (5.28, 7.66) dBi, respectively.

## ARTICLE INFO

**Handling editor:** Ivan A. Hashim

**Keywords:**
CRLH; Fractal curve; Hilbert structure; IDC; Metamaterial.

## ABSTRACT

With the development of communication systems, antennas of small size and high gain have become essential to keep up with the new challenges. The metamaterials made these challenges possible. In this paper, a new low-profile metamaterials-based array is designed. The array unit cell comprises a symmetric composite right left hand (CRLH) unit cell. A third-order Hilbert curve structure replaces the VIA, and aperiodic slots are introduced between the unit cells to enhance the overall performance. This design provides a significant improvement over the original design. CST MWS was used to stimulate the design. Gain and S11 are calculated to evaluate the antenna performance; a dual- bandwidth was achieved extended from (3.72 to 3.79) GHz and (6.99 to 8.55) GHz with maximum antenna gain equal to (5.28, 7.66) dBi, respectively. The antenna is characterized by its small size and high efficiency, making it suitable for Long-Term Evolution LTE, 5G, and satellite applications.

## 1. Introduction

With the development of communication systems and the increase of subscribers, finding antennas of small size, low cost, high efficiency, and scan capability was necessary. Therefore, these requirements have become an important area for researchers to find the latest techniques that provide solutions to these requirements [1-4].

Metamaterials (MTM) are considered technologies that have received particular attention in this field to control and manipulate electromagnetic waves to develop features and characteristics that are not available in nature, thus improving the overall performance[5, 6]. Negative constitutive parameters characterize the MTM, therefore called left-handed materials, as they generate a left-handed triad when spreading, which contrasts with the normal spread of other materials. Left-handed (LH) materials are not feasible due to the parasitic effects generated by the right-handed component [7].

A new type of MTM [CRLH-MTM] which combines the properties of LH- and right-handed (RH) materials, has been proposed by CALOZ[8]; it is used in many applications to provide high bandwidth and low loss in communication systems[9, 10]. The CRLH MTM consists of a series interdigital capacitor ($I_{DC}$) and a shunt stub inductor (SI), as shown in Figure 1.

CRLH is used in many different radio applications and microwave systems. In this section, a summary of the latest research findings was discussed. [11] This work analyzed and fabricated a reactive impedance surface (RIS)-MTM antenna. The antenna offers triple-band covering (1.66–1.72 GHz), (1.94–2.20 GHz), and (3.68–3.87 GHz) with gains equal to 1.6 dBi, 4.74 dBi, and 3.28 dBi, respectively. Dual-band circular polarization was obtained by combining the patch antenna with split-ring resonator (SLR) based RIS-MTM. The antenna can be used for different WiMAX, LTE, and satellite applications.[12]. Synthetic material is designed to achieve negative constitutive parameters over the operating frequency range. The material



http://doi.org/10.30684/etj.2022.132987.1160
Received 08 February 2022; Accepted 12 September 2022; Available online 27 December 2022
2412-0758/University of Technology-Iraq, Baghdad, Iraq

was tested for both gap and gap-less transitions. The material showed double negative parameters at low frequencies, and at high frequencies, the material showed double-positive parameters. As a result, the transition occurs at the same resonant frequency, thus providing a balanced CRLH. [13] CMOS technology-based 2D-CRLH was used to construct an antenna with a double polyimide layer of 500 $\mu_m$ thickness. A high bandwidth was achieved, ranging from 0.350–0.385 THz with a gain equal to 8.15dBi.

This paper proposes a new MTM antenna array to provide a good gain with a considerable spectrum across the operated bands. The proposed structure consists of a T-uniform CRLH and a 3rd-order Hilbert curve.

The dual-band antenna array operates from (3.72 to 3.79) GHz and (6.99 to 8.55) GHz, with maximum antenna gain equal to (5.2 and 7.66) dB, respectively. The S11 <= -20 dB along the operated bands.

Antenna geometrical details are discussed in the second section, where the design procedure and methodology used to arrive at the proposed design are presented. Results and simulation are discussed in section three, and a comparison between the proposed antenna and the latest research is discussed in the fourth section. In contrast, the design significance and originality are discussed in the fifth section, and finally, the conclusion is discussed in the last section.

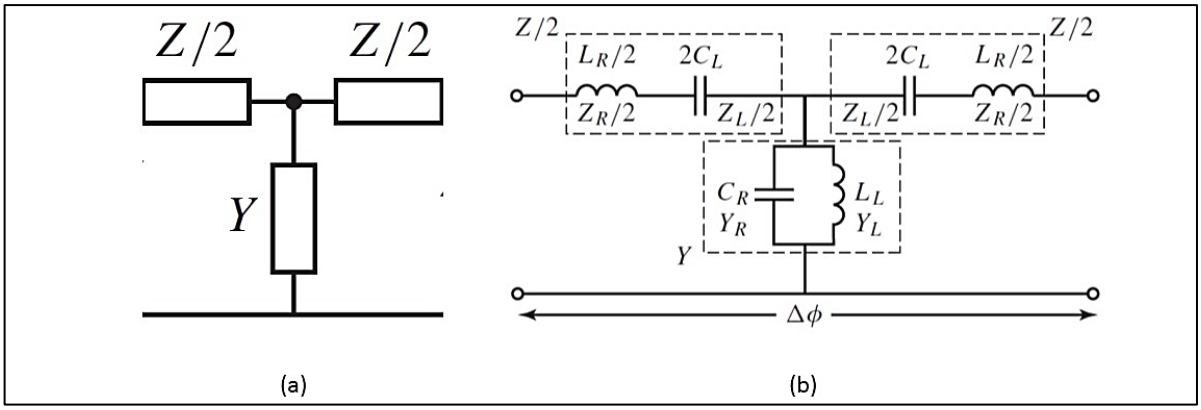


**Figure 1:** CRLH model (a) Symmetric cell (b) the equivalent model

## 2. Antenna Geometrical Details

The proposed antenna is implemented from two main parts based on the CRLH structure and Hilbert curve structure. Therefore, we denote the proposed design based on the following:

### 2.1 CRLH Details

Figure 2 shows a T-symmetric CRLH TL, represented by interdigital capacitors and stub inductors. The periodical separation between the CRLH unit cells provides significant enhancements to the proposed antenna gain-bandwidth product by suppressing the generated Skew waves from the edges of the substrates [14]. The interdigital capacitor is centered on the stub structure to realize a T-network of two impedance branches with 2CL and LR/2 values. The admittance branch with LL and CR values. The parameters of the CRLH unit cell are given in Table 1. The proposed T-network is represented by the equivalent circuit shown in Figure 2. The $I_{DC}$ and $S_I$ define left-handed parameters, while the RH parameters are formed due to the parasitic effects caused by the passage of current through the circuit. As the current pass through the IDC, a magnetic field is present, and a shunt inductor is generated, while the voltage gradient between the trace and ground plane causes the series capacitance.

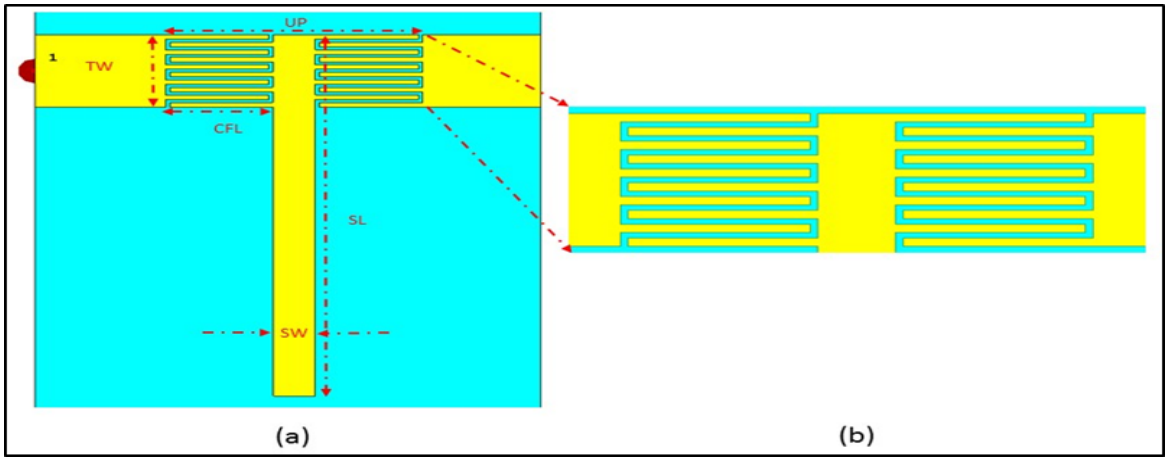


**Figure 2:** The proposed structure (a) T-uniform CRLH (b) IDC

**Table 1:** Design parameters

| No. | name | symbol | Value(mm) |
|---|---|---|---|
| 1 | Unit cell period | UP | 6.1 |
| 2 | Stub inductor length | SL | 12 |
| 3 | Stub inductor width | SW | 1 |
| 4 | Capacitor finger length | CFL | 2.55 |
| 5 | Capacitor finger width | CFW | 0.15 |
| 6 | Space between fingers | FS | 0.1 |
| 7 | TL width | TW | 2.4 |

## 2.2 Third-order Hilbert curve structure details

A Hilbert curve line is a continuous curve that fills a two-dimensional space with one-dimensional line segments. It is characterized by its simplicity and similarity [15]. The following equation gives Hilbert curve length:-

$$2^n - \frac{1}{2^n} \quad (1)$$

The length increases exponentially with n even though the total curve fills a square area of size one. The Hilbert curve configuration process is shown in Figure 3. at zero-order, the Hilbert curve is characterized by a U shape. This shape is repeated indefinitely for higher orders while maintaining the exact dimensions. In other words, the previous order curve replaces the higher vertices. In contrast, the lower vertices experience a rotation where the left vertex rotates 90° clockwise, and the right rotates 90° counterclockwise. For example, see Figure 3; at n=1, the fractal consists of four U shapes filling one area; at n=2, four 1st-order curves represent the fractal.

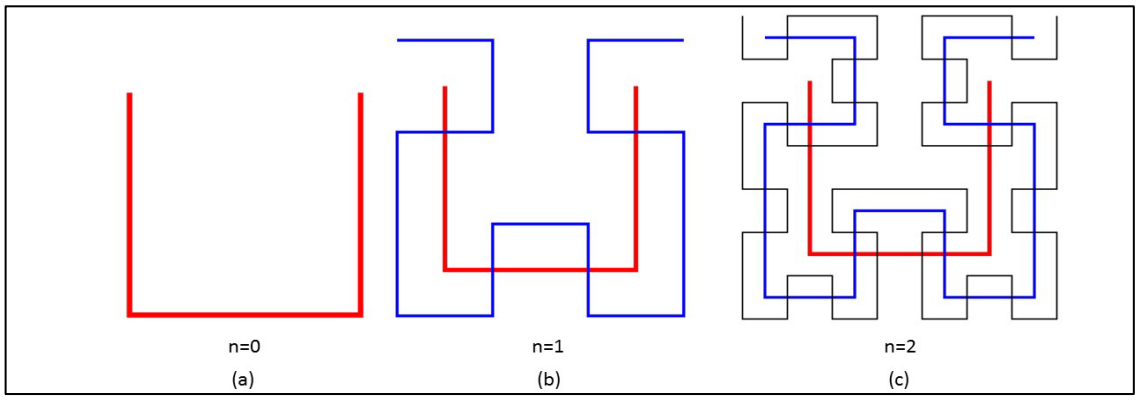


**Figure 3:** Hilbert configuration process

The proposed structure is constructed as a 3rd-order Hilbert shape fractal. The conducted Hilbert design is arranged as a 3×1 array placed in front of the CRLH-MTM unit cell to occupy an area of 13.69* 13.73 $mm^2$, as seen in Figure 3.

There is a direct proportion between area inductance and wire length. By increasing the wire length, the inductance can be improved, increasing the bandwidth while maintaining the miniaturization of the antenna [16]. Fractal structures are used in various applications to increase the operated band and create multiple resonances [17]. The dimension of the Hilbert unit cell is shown in Figure 4.

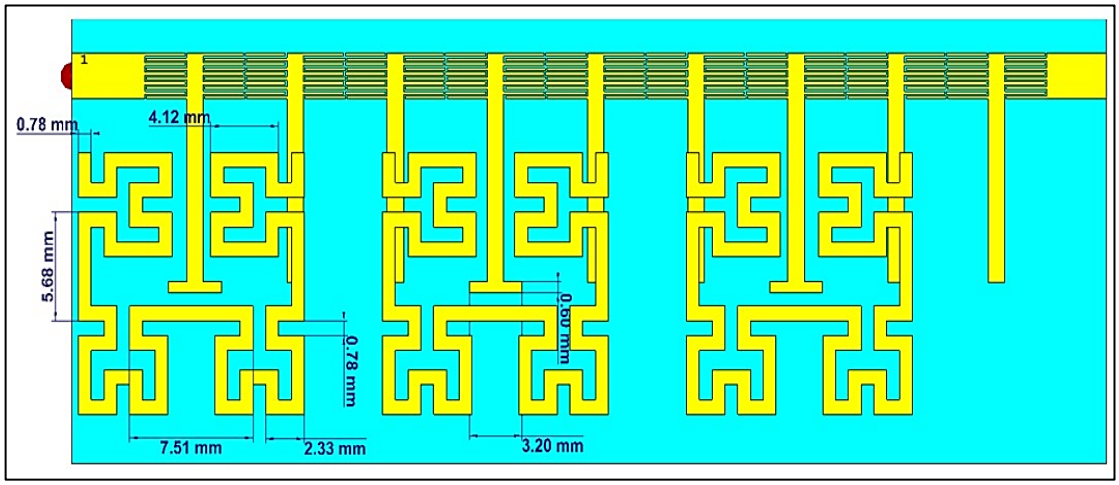


**Figure 4:** The proposed Hilbert curve structure

## 3. Results and Discussion

This section discusses the design process based on a numerical parametric study applied to arrive at the proposed antenna design. Therefore, a numerical simulation-based CST software tool package based on the finite integral technique is invoked as follows:

### 3.1 Before The Introduction of The Hilbert Curve Structure

#### 3.1.1 CRLH unit cell performance

A parametric study on the geometrical construction is performed to realize the effect of cell details. As seen in Figure 5, the proposed CRLH Model can be defragmented into three parts: a transmission line only, an interdigital capacitor with five fingers each, and a T-stub inductor to represent a capacitive tuner. Therefore, the $S_{11}$ is computed individually for each part, as shown in Figure 6. In such a study, the design is exciting with a 75Ω port.

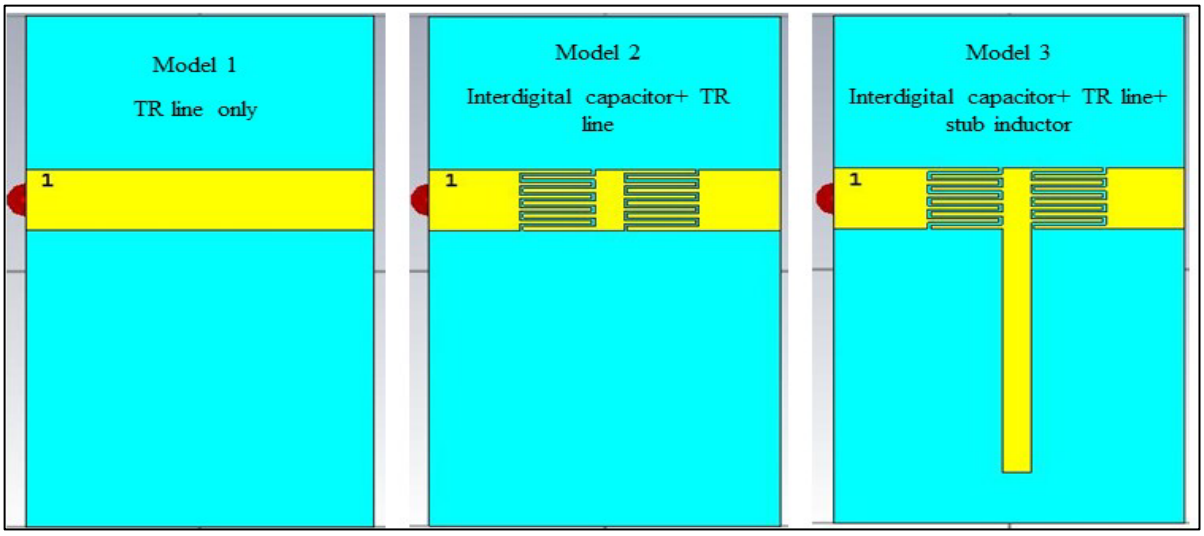


**Figure 5:** The proposed antenna geometrical details

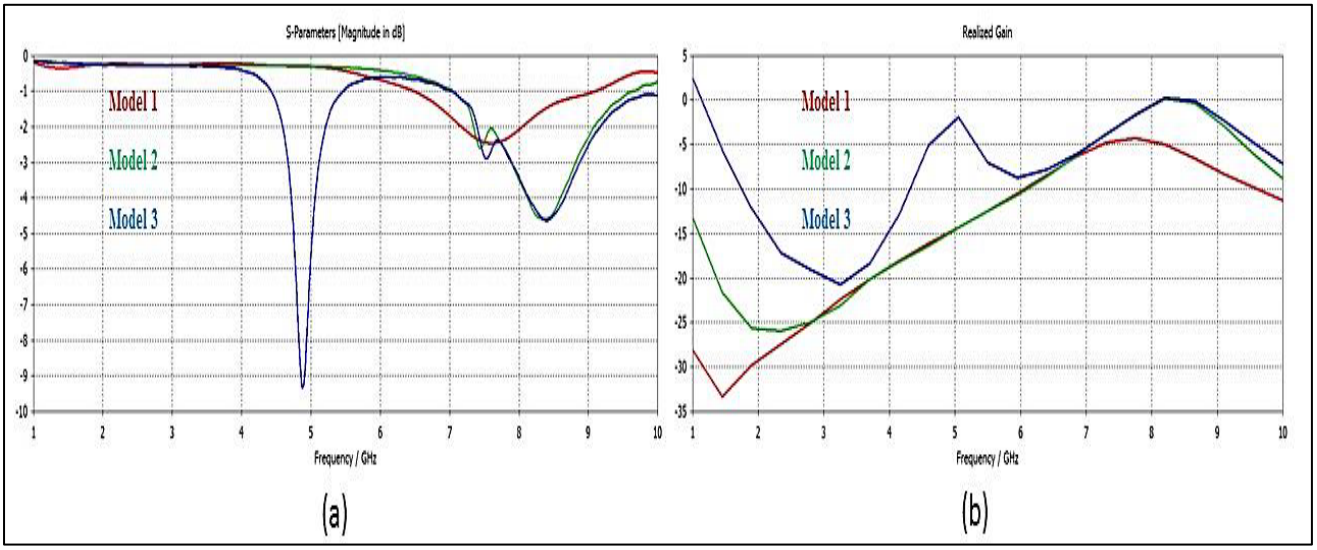


**Figure 6:** CRLH performance (a) S11 parameter (b) realized gain

#### 3.1.2 Antenna array performance

Figure 7 (a) shows the resulting antenna array with CRLH after arriving at the optimum unit cell dimensions. The antenna performance in terms of $S_{11}$ spectra and radiation patterns is presented in Figures 7(b) and 7(c). We found that the proposed antenna provides a triple bandwidth from (7 to 7.9) GHz, (8.2 to 8.6) GHz, and (9.2 to 9.3) GHz. the maximum antenna gain is equal to (7.13, 4.44, 1.35) dBi respectively.

The antenna radiation pattern at the resonance frequencies (7.6, 8.4, and 9.2) is given in Figure 7 (c). The current is concentrated in the middle; this is clear from the surface current flowing along the structure's surface as the current experiences the most negligible attenuation along with the interdigital capacitor, see Figure 8. The design procedures and basic parameters that significantly increase the gain and spectrum are briefly described in Figure 9.

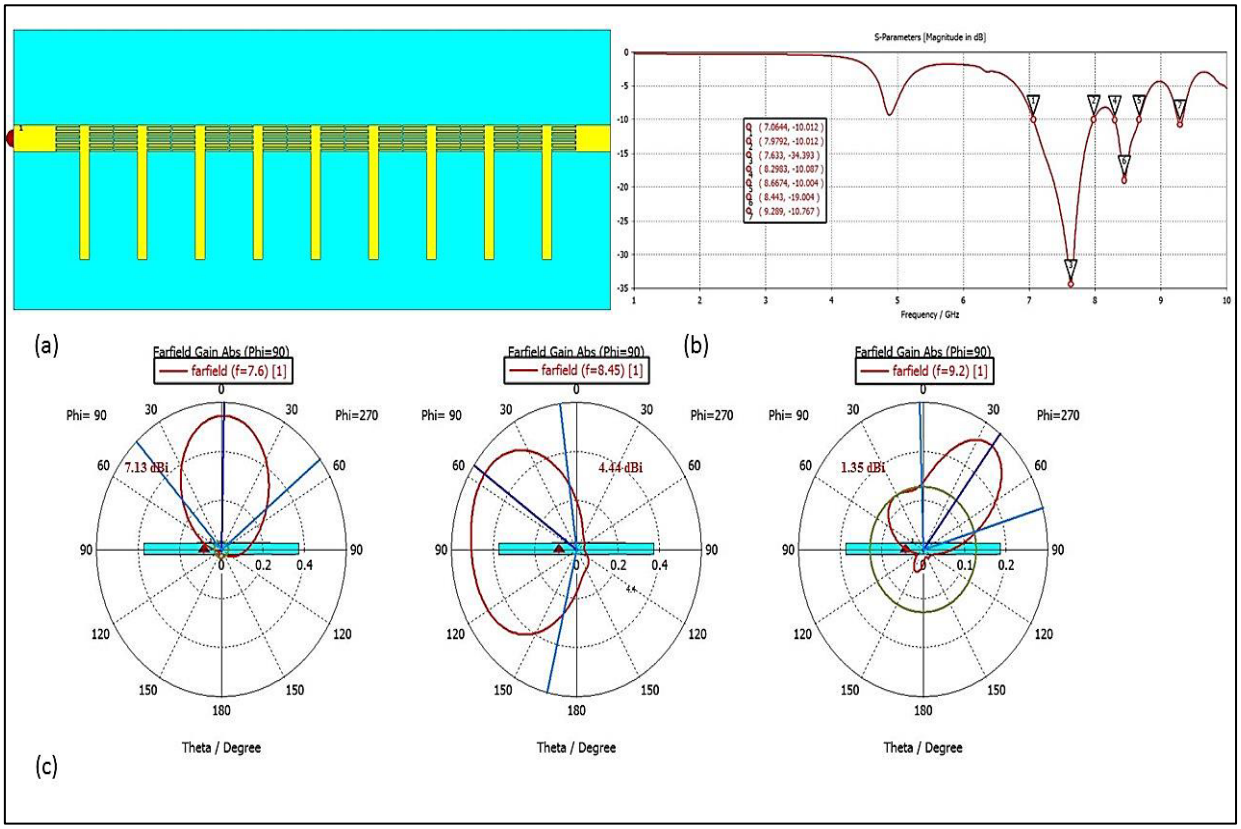


**Figure 7:** Array performance (a) CRLH antenna array (b) $S_{11}$ parameter (c) radiation patterns

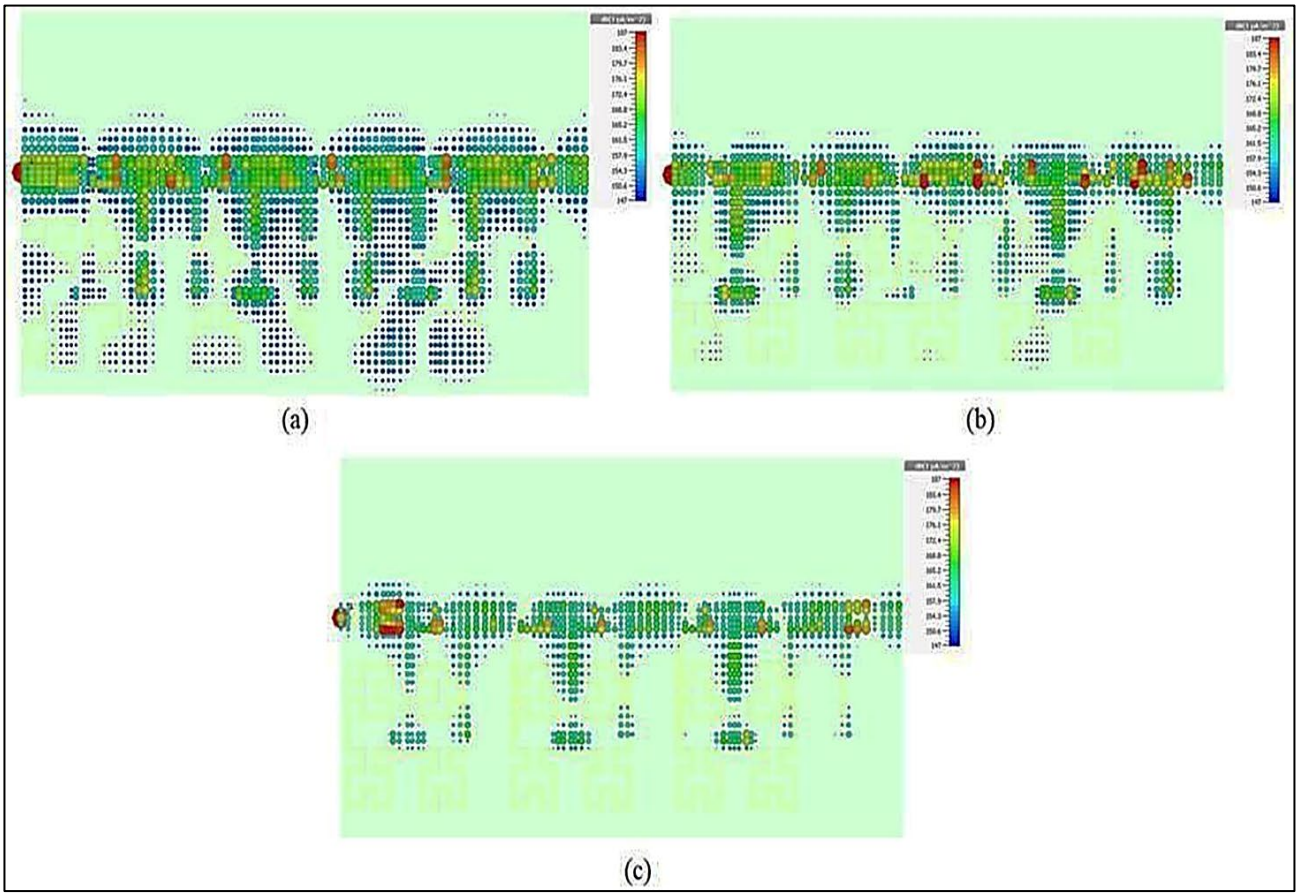


**Figure 8:** Surface current distribution SCD (a) at 7.9 GHz (b) at 8.4 GHz (c) at 9.2 GHz

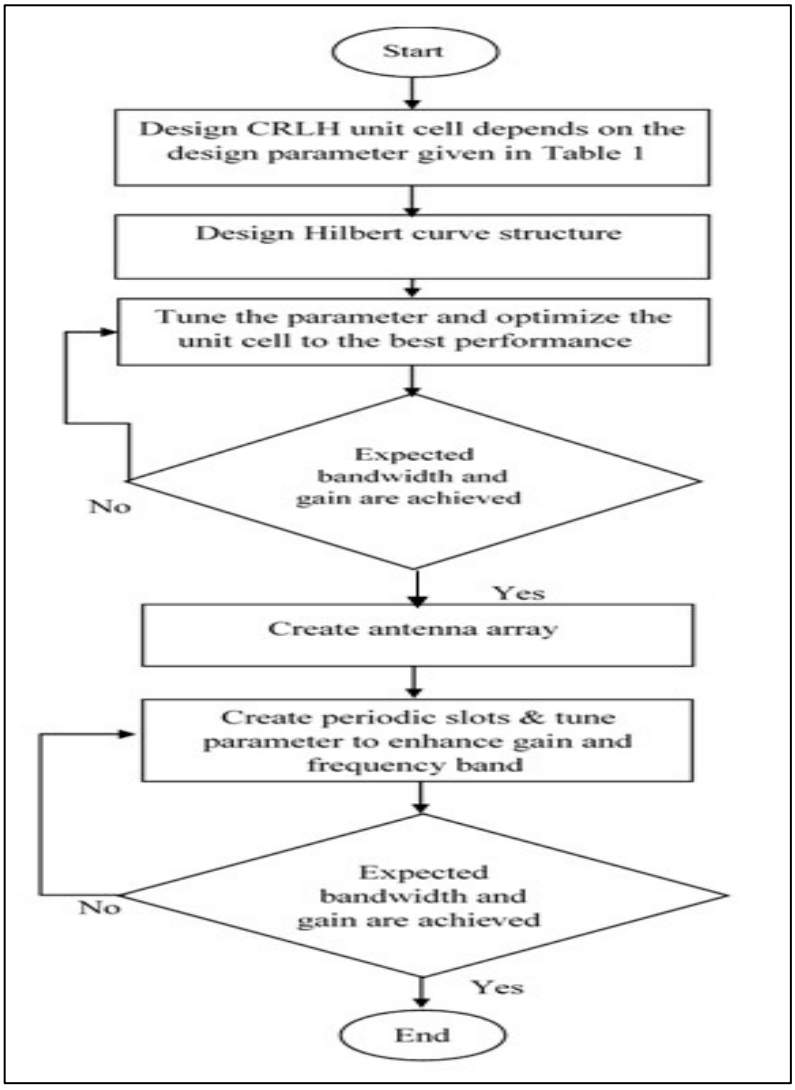


**Figure 9:** The design process

### 3.1.3 Antenna interdigital capacitor parametric study

A detailed parametric study was conducted on the number of fingers concerning the antenna transmission line. The fingers were changed from 1 to 5; antenna performance was calculated in each case for realized gain and $S_{11}$, see Figure 10. With the increase in finger numbers, the losses within the structure are reduced, resulting in better current distribution and, thus, greater gain and $S_{11}$.

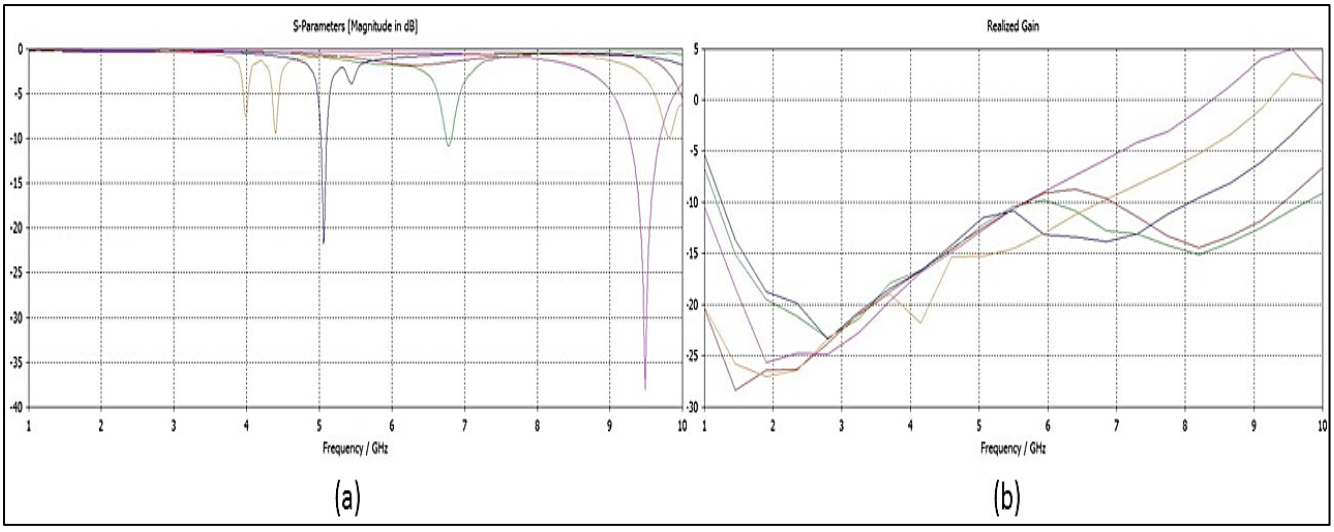


**Figure 10:** $I_{DC}$ parametric study (a) $S_{11}$ parameter (b) realized gain

### 3.1.4 Antenna array slots parametric study

To clarify the slots' role in the design and their importance in crystallizing the results in their final form. A study was conducted on the array with and without slots, $s_{11,}$ and realized gains were calculated in each case. It significantly obtains a wide bandwidth extending from 7 to 9.2 GHz and achieves high gain in the forward direction, in contrast to the band and gain achieved without slots; see Figure 11.

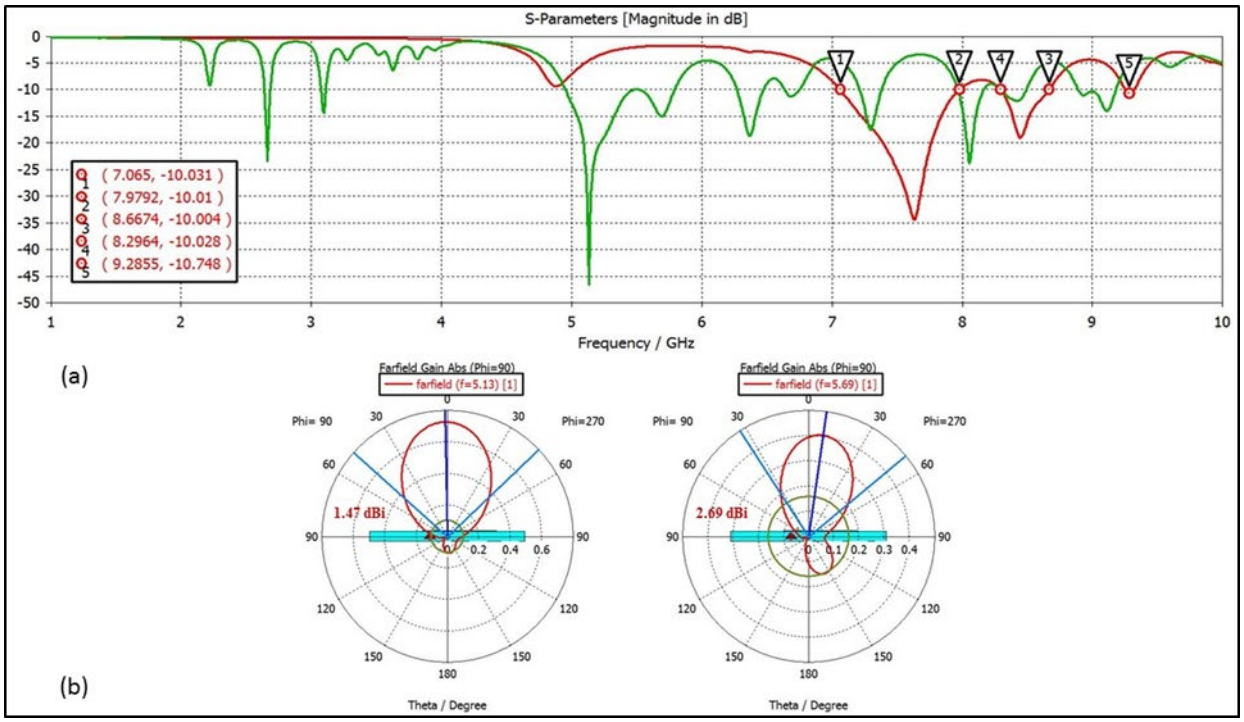


**Figure 11:** Periodic slots parametric study (a) S11 parameter (b) radiation pattern for the array without periodic slots

### 3.1.5 Stub inductor parametric study

In this section, the effect of the stub inductor on the array performance was studied, the stub dimensions were changed from 8 to 12 mm, and the gain and impedance bandwidth was calculated in each case, see Figure 12. The introduction of the stub creates a second resonance frequency at 6 GHz, where the voltage gradient between the ground and the copper develops a parasitic effect that produces a second resonance. As the length of the stub increases, this parasitic effect increases, reducing the matching and gain at some level, so dimension 12 is selected, giving the best result when combined with the Hilbert curve structure.

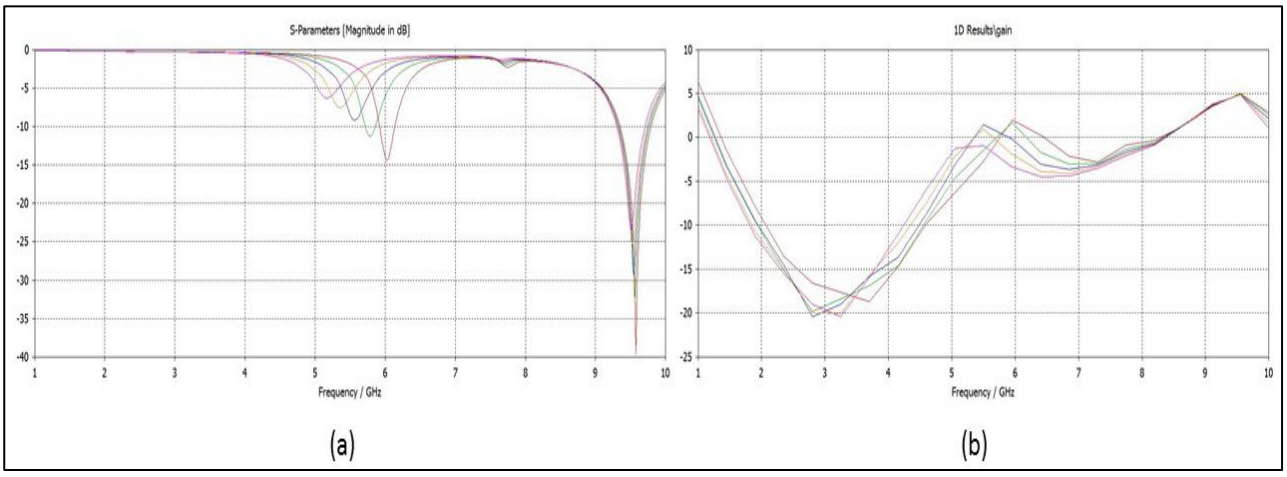


**Figure 12:** Stub-inductor parametric study (a) S11 parameter (b) realized gain

## 3.2 After the introduction of the Hilbert curve structure

This section studied the effect of the MTM Hilbert curve structure. The introduction of the proposed unit cell realizes several advantages: reducing the overall losses and enhancing performance without introducing extra size and complexity.

Furthermore, the Hilbert curve structure can introduce multiple resonance frequencies as it acts as a second radiator that allows the current to flow with tremendous energy. Moreover, each cell is considered balanced to the stub length where the capacitive effect is equal on both sides. Finally, the antenna inductance is increased due to the introduction of the Hilbert structure, thus compensating for the capacitance effect and expanding the operating frequency range.

The unit cell dimensions were modified and selected to be 13.7 * 13.7 to increase the effective electrical length of the unit cell. The T stub inductor and the Hilbert structure create resonance at 3.7 GHz with good matching. In addition, the Hilbert cell represents a shading area in self-power wireless devices. The current activates the cell, and the energy is coupled to the cell through SI. Figure 13 shows the s11 and gain after introducing the Hilbert structure

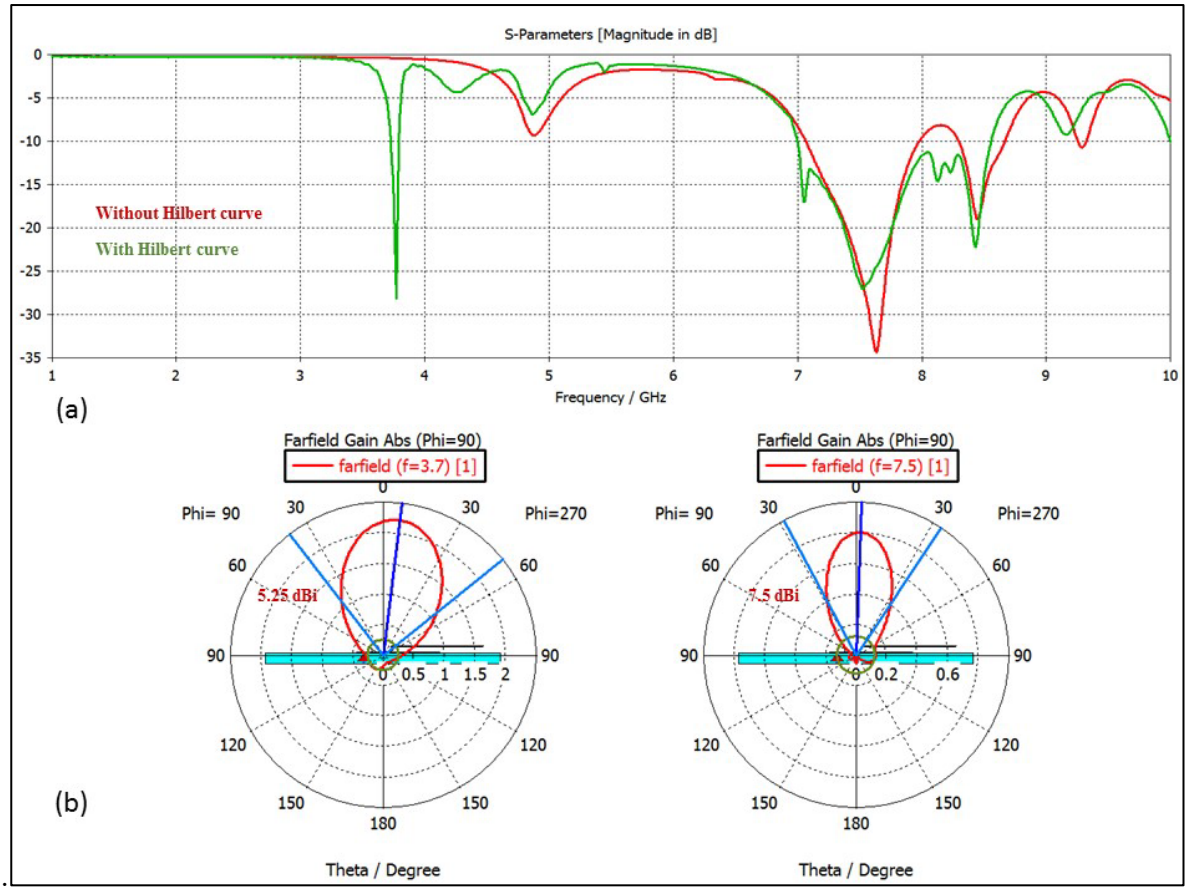


**Figure 13:** Hilbert curve parametric study (a) S11 parameter (b) radiation pattern

## 4. Comparisons With the Latest Publications

The following Table2 gives insight and compares with the relative research findings in this field:-

It was found that the proposed antenna provides high gain with excellent impedance-matched bandwidth in the first and second bands, respectively. These characteristics make the antenna a good candidate for applications such as radar, mobile phones, commercial wireless LANs, and the 5G sub-6 GHz network.

**Table 2:** A comparison with the relative interest

| size | spectrum range (GHz) | maximum gain (dBi) | Bands | Ref. |
|---|---|---|---|---|
| Not-mentioned | 3 to 9 | 5 | Wide band | [18] |
| 1.31λ * 14.45λ | 5.8 | 23.6 | Single-band | [19] |
| 1.4λ * 0.79λ | 5,5.8,6.3 | 9.99 | Trible band | [20] |
| 2.68λ * 1.38λ | 1.8-2.6 | 12.1 | wide band | [21] |
| 1.65λ0.97λ | 2.5 | 4.42 | Single-band | [22] |
| 7.9λ* 1.12λ | 6.9-13.5 | 15.2 | wideband | [23] |
| 5.15λ ×0.66λ ×0.03λ | 8 to 12 | 11 | Wide band | [24] |
| 0.08 λ× 0.12 λ× 0.007 λ | 8-15 | 7, 10.4 | Wide band | [25] |
| Not-mentioned | 7.6–10.6 | 10 | dual-band | [26] |
| 0.6λ* 1.61λ | 3.7, 6.99-8.5 | 5.28 , 7.66 | Dual-band | This work |

## 5. Discussion of the Significance and Novelty of The Proposed Structure

The novelty of the design is a nine-cell MTM -array design that achieves a gain equal to 29- cells of the original design. The VIA that causes high losses has been replaced with a fractal that achieves high gain using an inexpensive substrate [FR-4 ]

compared to the expensive substrate [Roger substrate] design. The periodic slots resulted in a wideband extended from 6.9 to 8.55 GHz with $S_{11}$ less than -20 dB. As far as we know, it was not previously used in the design of CRLH MTM. Furthermore, The study evidence shows that such antenna gain-bandwidth enhancement is improved by: reducing the influence of via losses, the capacitive losses caused by the ground metallization, and the suppression of surface waves by the Hilbert curve.

The importance of design lies in designing a compact, low-complexity, broadband, high-gain antenna suitable for wireless applications. In addition, the design represents the beginning of creating antennas with various developing performances such as beamforming through different technologies such as electronic, mechanical, or any other technology.

## 6. Conclusion

This paper presents a detailed study on designing a new MTM antenna array. First, a regular microstrip line was generated, and left-handed components were added to form a CRLH-MTM structure. Finally, the Hilbert curve has been added to compensate for the VIA. As a result, The antenna Operates in dual-bands with good gain and $s_{11}$, which is characterized by its simplicity, making it suitable for wireless devices.

### Author contribution

All authors contributed equally to this work.

### Funding

This research received no specific grant from any funding agency in the public, commercial, or not-for-profit sectors.

### Data availability statement

The data that support the findings of this study are available on request from the corresponding author.

### Conflicts of Interest

The authors declare no conflict of interest.

## References

**[1]** Y. S. Mezaal, S. F. Abdulkareem, J. K. Ali, A dual-band printed slot antenna for WiMAX and metrological wireless applications, Adv. Electromagn., 7 (2018) 75-81. https://doi.org/10.7716/aem.v7i3.765

**[2]** B. S. Bashar, M. M. Ismail, A.-S. M. Talib, Optimize Cellular Network Performance Using Phased Arrays, in IOP Conf. Ser.: Mater. Sci. Eng. IOP Publishing, 870,2020,012128. https://doi.org/1088/1757-899X/870/1/012128

**[3]** E. S. AHMED, Design of CPW Fed Two Layered Rectangular Dielectric Resonator Antenna for 5G Mobile Communications, J. Duhok Univ., 23(2020)754-766.

**[4]** A. Q. Hameed, S. Goli, Z. J. Oleiwi, 5G: MIMO BDMA SYSTEM TRENDS AND TECHNOLOGY, QALAAI ZANIST J., 2 (2017) 1-15. https://doi.org/10.25212/lfu.qzj.2.2.01

**[5]** A. A. Althuwayb, MTM-and SIW-inspired bowtie antenna loaded with AMC for 5G mm-wave applications, Int. J. Antennas Propag., 2021 (2021) 7. https://doi.org/10.1155/2021/6658819

**[6]** Chindhi, P.S., Kalkhambkar, G.B., Rajani, H.P., Khanai, R. 2022. A Brief Survey on Metamaterial Antennas: Its Importance and Challenges, vol. 792. pp 425–432. Springer, Singapore.. https://doi.org/10.1007/978-981-16-4625-6_41

**[7]** S. Lee et al., Design , Characterization of VHF Band Small Antenna Using CRLH Transmission Line and Non-Foster Matching Circuit, Appl. Sci. 10 (2020) 6366. https://doi.org/10.3390/app10186366

**[8]** C. Caloz ,T. Itoh, Novel microwave devices and structures based on the transmission line approach of meta-materials, IEEE MTT-S Int. Microw. Symp. Dig., 2003, Philadelphia, PA, USA, 1, 2003, 195-198. https://doi.org/10.1109/MWSYM.2003.1210914

**[9]** A. H. Jabire et al., Metamaterial based design of compact UWB/MIMO monopoles antenna with characteristic mode analysis, Appl. Sci., 11(2021)1542. https://doi.org/10.3390/app11041542

**[10]** A. Garhwal et al., Integrating metamaterial antenna node and LiFi for privacy preserving intelligent COVID-19 hospital patient management, Cognit. Comput., 1-14, 2021. https://doi.org/10.1007/s12559-020-09778-6

**[11]** M. Ameen ,R. K. Chaudhary, Dual-layer and dual-polarized metamaterial inspired antenna using circular-complementary split ring resonator mushroom and metasurface for wireless applications, AEU - Int. J. Electron. Commun., 113(2020)152977. https://doi.org/10.1016/j.aeue.2019.152977

**[12]** H. Singh, A. Gupta, S. Bakshi, and N. Mittal, Designing and analysis of non-symmetric dual layer CRLH metamaterial, J. Magn. Magn. Mater., 538(2021)168269. https://doi.org/10.1016/j.jmmm.2021.168269

**[13]** M. Alibakhshikenari, B. S. Virdee, C. H. See, R. A. Abd-Alhameed, F. Falcone, and E. Limiti, High-gain metasurface in polyimide on-chip antenna based on CRLH-TL for sub-terahertz integrated circuits, Sci. Rep., 10 (2020) 1-9. https://doi.org/10.1038/s41598-020-61099-8

**[14]** B. Mohamadzade, A. Lalbakhsh, R. B. Simorangkir, A. Rezaee, and R. M. Hashmi, Mutual coupling reduction in microstrip array antenna by employing cut side patches and EBG structures, Prog. Electromagn. Res. M, 89 (2020)179-187. https://doi.org/10.2528/PIERM19100703

**[15]** T. Li, J. Zhang, B. Cheng, X. Lei, Z. Xu, J. Gao, Compact Wideband Dual-Frequency Antenna Based on a Simplified Composite Right/Left-Handed Transmission Line with Hilbert Curve Loading, Int. J. Antennas Propag., 2019 (2019) 8. https://doi.org/10.1155/2019/7380621

**[16]** I. S. Bangi, J. S. Sivia, Minkowski and Hilbert curves based hybrid fractal antenna for wireless applications, AEU - Int. J. Electron. Commun., 85(2018) 159-168. https://doi.org/10.1016/j.aeue.2018.01.005

**[17]** X. Ran, Z. Yu, T. Xie, Y. Li, X. Wang, and P. Huang, A novel dual-band binary branch fractal bionic antenna for mobile terminals, Int. J. Antennas Propag., 2020 (2020) 9. https://doi.org/10.1155/2020/6109093

**[18]** B.-F. Zong, H.-Y. Zeng, F. Wu, G.-M. Wang, L. Geng, Wide-Angle Frequency-Scanning Array Antenna Using Dual-Layer Finger Connected Interdigital Capacitor Based CRLH Unit Cell, IEEE Access, 9 (2020) 35957-35967. https://doi.org/10.1109/ACCESS.2020.2997256

**[19]** Q. Bai , J. Wang, Composite right/left-handed substrate integrated waveguide leaky-wave antenna array with low sidelobe level and high gain, 2017 7th IEEE International Symposium on Microwave, Antenna, Propagation, and EMC Technologies (MAPE), Xi'an, China, 2017, 37-40. https://doi.org/10.1109/MAPE.2017.8250790

**[20]** A. A. Ibrahim, M. A. Abdalla, Z. Hu, Compact ACS-fed CRLH MIMO antenna for wireless applications, IET Microw. Antennas Propag., 12 (2018) 1021-1025. https://doi.org/10.1049/iet-map.2017.0975

**[21]** D. Ren , J. H. Choi, Full-sphere frequency scanning array antenna based on passive dual-band CRLH series integrated feeding network, 2019 IEEE MTT-S International Microwave Symposium (IMS), Boston, MA, USA, 2019, 1462-1465. https://doi.org/10.1109/MWSYM.2019.8700839

**[22]** A. A. Abdel Aziz, A. A. Ibrahim, M. A. Abdalla, Tunable array antenna with CRLH feeding network based on graphene, IETE J. Res., 68 (2019) 1713-1721. https://doi.org/10.1080/03772063.2019.1666751

**[23]** R. Noumi, J. Machac, A. Gharsallah, Complex beam steering from substrate integrated waveguide leaky wave antenna array, Int. J. RF Microw. Comput. Aided Eng., 28 (2018) e21548. https://doi.org/10.1002/mmce.21548

**[24]** K. T. Chandrasekaran, M. Ong, A. Alphones, and M. F. Karim, A consistently high gain frequency scanning antenna for portable low-profile beamforming applications, in 2018 Asia-Pacific Microwave Conference (APMC), 2018 Asia-Pacific Microwave Conference (APMC), Kyoto, Japan, 2018, 1597-1599. https://doi.org/10.23919/APMC.2018.8617265

**[25]** R. Sonak, M. Ameen, R. K. Chaudhary, CPW-fed electrically small open-ended zeroth order resonating metamaterial antenna with dual-band features for GPS/WiMAX/WLAN applications, AEU - Int. J. Electron. Commun., 104 (2019) 99-107. https://doi.org/10.1016/j.aeue.2019.03.017

**[26]** R. Agarwal, R. Yadava, S. Das, A Multilayered SIW-Based Circularly Polarized CRLH Leaky Wave Antenna, IEEE Trans. Antennas Propag., 69 (2021) 6312-6321. https://doi.org/10.1109/TAP.2021.3082618